

# Effect of the deposition parameters on the voiding propensity of solder joints with Cu electroplated in a Hull cell

F. Wafula · Y. Liu · L. Yin · P. Borgesen ·  
E. J. Cotts · N. Dimitrov

Received: 5 November 2010 / Accepted: 4 February 2011 / Published online: 26 February 2011  
© Springer Science+Business Media B.V. 2011

**Abstract** A quantitative study of the impact of key Cu plating parameters on the voiding propensity of solder joints with Cu electroplated in a commercially available plating solution (CAPS) is performed first on 0.3 cm<sup>2</sup> Cu rotating disk electrode. It is shown that similar to samples plated in a generic plating solution (GPS) containing bis(3-sulfopropyl) disulfide, polyethylene glycol, and Cl<sup>-</sup> ions, void-prone samples are deposited predominantly at higher overpotentials, in the range from positive to -0.20 V. In the second part, a Hull cell with 46 cm<sup>2</sup> cathode is used to scale up the voiding study in both, GPS and CAPS. It is demonstrated that plating conditions could be chosen in a way to generate both, void-prone and void-proof Cu on the same cathode panel. Thus, the controlled voiding propensity illustrated for the first time in a prototype of industrial Cu plating helps in realizing the sporadic nature of the voiding phenomenon.

**Keywords** Cu electroplating · Impurity incorporation · Solder joints · Voiding · Hull cell

## 1 Introduction

The lead-free solders with Cu pad structures being currently used have been reported to suffer from occasional premature failure under shock loading [1–4]. The cause for the failure was determined to be associated with the sporadic Kirkendall void formation in the intermetallic compound (IMC) (i.e., Cu<sub>3</sub>Sn) of the solder joint during thermal aging. The formation and growth of these voids have been shown to be strongly correlated with the quality of electroplated copper samples that were soldered onto [4]. This has been the cause of great concern to the microelectronics industry that deals with Cu electrodeposition from the acidic copper solutions with key applications in the interconnections of the printed circuit board (PCB) and integrated circuit (IC) [5, 6].

A systematic study on voiding during the era of Pb-free manufacturing suggested that voiding in Cu<sub>3</sub>Sn was independent of solder alloy Ag and Cu composition, flux selection, soldering process parameters, and surface coatings on electroplated Cu, e.g., immersion Ag, immersion Sn etc. [7]. Although a study by Kim et al. has shown that the addition of sulfide-forming elements (Cr, Mn, and Zn) as a third element to Sn-3.5Ag solder suppressed Kirkendall voids, other negative effects of the addition of third element to the interface, apart from the positive drop reliability improvement, may result [8].

Interestingly, studies done where soldering was performed on high purity wrought Cu foils followed by a thermal aging treatment showed an insignificant level of

---

F. Wafula · N. Dimitrov  
Department of Chemistry, State University of New York  
at Binghamton, Binghamton, NY 13902-6000, USA

Y. Liu · E. J. Cotts · N. Dimitrov (✉)  
Materials Science Program, State University of New York  
at Binghamton, Binghamton, NY 13902-6000, USA  
e-mail: dimitrov@binghamton.edu

L. Yin  
Advanced Research on Electronics Assembly, Consortium,  
Universal Instruments Corporation, Conklin, NY 13748, USA

P. Borgesen  
Department of Systems Science and Industrial Engineering,  
State University of New York at Binghamton, Binghamton,  
NY 13902-6000, USA

E. J. Cotts  
Department of Physics, State University of New York  
at Binghamton, Binghamton, NY 13902-6000, USA

voiding in the interfacial  $\text{Cu}_3\text{Sn}$  phase [9, 10]. Other studies reported by Kim et al. were done to investigate the effects of residual S on Kirkendall void formation, where Cu films were electroplated with or without bis(3-sulfo-propyl) disulfide (SPS) in the plating bath [11, 12]. The reported results show that the addition of SPS strongly affected the characteristics of Kirkendall void formation as voids were predominantly distributed near the  $\text{Cu}_3\text{Sn}/\text{Cu}$  interface with SPS, but randomly distributed in the  $\text{Cu}_3\text{Sn}$  layer without SPS. The authors proposed that S segregation to the  $\text{Cu}/\text{Cu}_3\text{Sn}$  interface lowered the interface energy and thereby the free energy barrier for Kirkendall void nucleation [11, 12].

To assess the quality of electroplating to the voiding propensity, studies reported by our research group have shown that voiding in the IMC  $\text{Cu}_3\text{Sn}$  can be “turned on” and “turned off” by monitoring the factors that govern the electrodeposition of Cu from the acidic copper sulfate solution that are largely responsible for the impurity incorporation termed to be the primary cause to void evolution in the IMC [13–15]. The impurities associated with voiding came from the additives used in the Cu electrodeposition [13, 14], i.e., polyethylene glycol (PEG), SPS, and the chloride ions ( $\text{Cl}^-$ ) that are indispensable in today’s industrial acid Cu electroplating solution [6, 16, 17]. The effect of solution composition, deposition rate, deposition potential, solution temperature, and solution aging on the voiding propensity in the Cu solder joint have been investigated [14, 15]. The incorporation of these impurities took place at different current densities when  $\text{PEG} + \text{Cl}^-$  or  $\text{SPS} + \text{PEG} + \text{Cl}^-$  were used as additives [13, 14]. When  $\text{PEG} + \text{Cl}^-$  was added to Cu plating bath, characterization of accordingly grown Cu deposits using the secondary ion mass spectroscopy (SIMS) showed that there was a substantial incorporation of PEG at current densities of 10–40  $\text{mA cm}^{-2}$ , while for a bath that contained  $\text{SPS} + \text{PEG} + \text{Cl}^-$ , an increase in the SPS in the deposit was registered in the range 0.5–5.0  $\text{mA cm}^{-2}$  [13, 14]. Accordingly, higher voiding propensity was found in Cu deposits with a higher impurity level. Also, with Cu plating in the presence of  $\text{SPS} + \text{PEG} + \text{Cl}^-$ , high solution temperatures favor the S incorporation at low overpotentials resulting to formation of a thick layer of voiding in the  $\text{Cu}_3\text{Sn}$  as the catalytic effect of  $\text{Cl}^-$  becomes insignificant in the  $\text{PEG} + \text{Cl}^-$  incorporation due to precipitation of the  $\text{CuCl}$  [15]. This clearly shows strong dependencies of voiding propensity on the plating conditions.

A further and comprehensive analysis relied on the experimentally obtained potential-current-temperature results with respect to the voiding propensity helped to identify that plating potential is the determining parameter on the voiding propensity. We established the ranges of

overpotentials where either “void-prone” or “void-free” Cu could be deposited in two acidic Cu plating solutions containing different additive combinations. As a result, we reported that in the presence of  $\text{SPS} + \text{PEG} + \text{Cl}^-$ , voiding is observed in the overpotential range more positive than  $-0.11$  V versus Cu pseudo reference electrode regardless of the temperature and current density combinations employed; whereas in the presence of  $\text{PEG} + \text{Cl}^-$ , voiding is observed in the overpotential range more negative than  $-0.23$  V [15, 18]. While this analysis undoubtedly helps in the prediction and control of voids in the  $\text{Cu}_3\text{Sn}$  IMC when soldering is done on electroplated Cu films, more research is needed to address the specificity of the voiding problem in the realm of the industrial Cu plating.

The study described herein consists of two relatively separate activities both aimed at elaborating on specific issues associated with the industrial plating. In the first part, the analysis of the correlation between plating parameters and voiding propensity developed in [15] is extended to Cu electrodeposited in commercially available plating solutions (CAPS) in rotating disk electrode (RDE) configuration at either constant current density while varying temperature or at constant temperature with a variation of the current density. The resultant *current-voltage-temperature* ( $i-\eta-T$ ) dependencies are used in identifying the potential ranges for generating void-proof or void-prone Cu samples using CAPS. In the second part, scaled up Cu plating experiments founded on previously analyzed plating scenarios and carried out in a Hull cell (volume of 267 mL) are aimed at examining regions of the surface where supposedly “void-proof” and “void-prone” Cu co-exist in a controlled way on the same cathode panel. This part of the study is done using both the CAPS and our generic plating solution (GPS) with  $\text{PEG} + \text{Cl}^-$  and  $\text{SPS} + \text{PEG} + \text{Cl}^-$  additives. The analysis of the results obtained will be important in controlling the sporadic voiding in  $\text{Cu}_3\text{Sn}$  IMC under industrially relevant Cu plating conditions.

## 2 Experimental

Electrodeposition of Cu from (i) GPS having  $\text{SPS} + \text{PEG} + \text{Cl}^-$  and  $\text{PEG} + \text{Cl}^-$  additives and (ii) CAPS with additives A and B representing proprietary formulations undisclosed by the vendor, was carried out in a standard 267-mL Hull cell (two-electrode setup) while a beaker (100 mL) with CAPS only (similar study with GPS was reported in [15, 18]) was used for Cu electrodeposition in RDE configuration at a constant rotation speed of 50 rpm. More details on the additives, A and B, will be provided later in this study.

## 2.1 Electrodeposition in a three-electrode cell using RDE

Cu disks (99.99%, Advent Research Materials, Ltd.), 6-mm diameter and 1-mm thickness, were used as working electrodes (plating substrates). Before the plating process, the electrodes were mechanically polished on cloths soaked with different sizes of alumina slurry (Buehler) down to 0.05  $\mu\text{m}$ . Right before the plating, the mechanically polished Cu disks were electropolished following a procedure described in a previous study [19]. Next, the Cu surface was thoroughly rinsed with Barnstead Nanopure<sup>®</sup> water ( $R > 18.2 \Omega \text{ cm}$ ) and dried with high purity  $\text{N}_2$  gas (less than 1 ppb oxygen, CO,  $\text{CO}_2$ , and moisture content). Right after that, the sample was mounted onto a holder of a rotating disk setup (PINE Instruments Rotator with MSPX Speed Control) to be used as a working electrode. A constant current density was applied using potentiostat/galvanostat Princeton Applied Research, EG&G, Model 273. A phosphorized Cu anode (Kocour, 0.04–0.06% P) serving as a counter electrode was prepared as outlined in part 2.2 below. A Cu wire (99.99%, Surepure Chemetals), pre-etched in a 1:3 mixture of  $\text{HNO}_3$  and  $\text{H}_2\text{O}$  and rinsed with Barnstead Nanopure<sup>®</sup> water, served as a pseudo reference electrode (*pre*). All potentials in this study are reported versus the Cu *pre* as overpotentials  $\eta = E - E_{\text{Cu}^{2+}/\text{Cu}}$ . The GPS used was formulated as described in Sect. 2.2 below. Each plating experiment was aimed at producing at least a 10- $\mu\text{m}$ -thick Cu layer so that the deposition time was calculated based on the constant current density applied in each particular experiment. The specific plating conditions for each experiment are described in Sect. 3 and in the *figure legends*. After each plating event, the sample was rinsed with Barnstead Nanopure<sup>®</sup> water and dried with high purity  $\text{N}_2$ . Finally, the sample was subjected to soldering, heat-treatment, and characterization as outlined below.

## 2.2 Electrodeposition in the Hull cell

Cu sheet, 10 cm  $\times$  7.5 cm, was used as a cathode panel. Before usage, the panel was dipped in 10 vol% sulfuric acid for about 3 s for removal of traces of oxide, rinsed with Barnstead Nanopure<sup>®</sup> water, and dried with high purity nitrogen gas. One side of the cathode panel was masked using nail polish to allow copper plating only on the side with mirror like finish. Acetone was used to rinse off carefully the nail polish not to contaminate the electrodeposited Cu film after Cu deposition. The anode used in this experiment was phosphorized copper (Kocour, 0.04–0.06% P) measuring 6.5  $\times$  6.0  $\text{cm}^2$  pretreated by etching in 8 M nitric acid and rinsing thoroughly with Barnstead Nanopure<sup>®</sup> water. The phosphorized Cu anode was prepared (filmed) before each

plating experiment. The filming procedure was developed according to recommendations described previously [14]. Since the effective anode area was to be higher to have anodic and cathodic efficiencies in the ratio of 1:1, a ridged anode was used in this experiment. The GPS plating solution was formulated in our laboratory and consisted of 0.26 M  $\text{CuSO}_4 \cdot 5\text{H}_2\text{O}$  (Sigma-Aldrich), 2 M  $\text{H}_2\text{SO}_4$  (doubly distilled, GFS), 1.13 mM HCl (doubly distilled, Sigma-Aldrich), 0.02 mM PEG ( $M_w$  4,000, Fluka), and 0.01 mM SPS (Rachig). All chemicals were used as-received from the corresponding vendors. Desired solution compositions were achieved by mixing the above chemicals at the concentration values presented above. The CAPS obtained from an undisclosed vendor was used in the second part of the experiment that included use of base copper plating solution and two additives A and B added in the ratio 1:4. In the Hull cell setup, the constant current (Kocour Model 5D) applied was 0.5 A for the PEG +  $\text{Cl}^-$  system, while for the SPS + PEG +  $\text{Cl}^-$  (GPS) and the CAPS, 0.3 and 0.1 A was used, respectively. All currents were chosen according to previously published studies [13–15] in a way to provide conditions for co-existence of void-free and void-prone Cu in one plated sample. After each plating event, the cathode panel was rinsed with Barnstead Nanopure<sup>®</sup> water and dried with high purity  $\text{N}_2$ . Finally, the sample was subjected to soldering, heat-treatment, and characterization.

## 2.3 Soldering, reflow, heat-treatment, and characterization

The soldering of the Cu samples was carried out in a 10-zone reflow oven (Vitronics Soltec XPM1030 N) in nitrogen atmosphere. Before reflow, Sn(3.0)Ag(0.5)Cu solder spheres with 0.5-mm diameter were placed onto the plated Cu panel at equal distance vertically across the panel with a Kester TSF-6522 soldering flux. The solder reflow profile was typical of lead-free soldering and had a peak temperature of 260  $^\circ\text{C}$  and a time above liquidus of 60 s. Soldered panels were then isothermally aged in air at 175  $^\circ\text{C}$  for 1 week (for SPS + PEG +  $\text{Cl}^-$ , PEG +  $\text{Cl}^-$  and CAPS). After isothermal aging, pieces to be mounted in the mixture of resin epoxy and hardener were cut out horizontally from the panel. The samples were then cross-sectioned and polished by standard metallurgical preparation procedures, where the final polishing step was performed with a 0.02- $\mu\text{m}$  colloidal silica suspension to give a better phase contrast. The thickness of Cu deposit and the interfacial voiding levels were inspected by scanning electron microscopy (SEM). Images were taken by a Zeiss EVO50XVP SEM at 4,000 $\times$  magnification under the backscattered electron mode to show phase contrast. The resolution at this magnification was 0.048  $\mu\text{m pixel}^{-1}$ . Calculations of the locally operating current on each spot

are hereby performed knowing the deposition duration time and using the SEM images of the interface to measure the deposit thickness.

### 3 Results and discussion

#### 3.1 Voiding behavior of CAPS plated Cu in RDE configuration

In a recent study, an approach based on the analysis of the  $i$ - $T$ - $\eta$  curve in terms of the voiding propensity was developed for understanding of the impact of the plating conditions on the voiding behavior of Cu samples. To date, the applicability of such approach has been tested only for Cu samples grown in GPS, which is composed from solutions proposed in literature for superconformal electroplating of Cu [15, 18]. Since the relevance of GPS to industrially used Cu plating solutions is overall unknown, it is a challenge to draw specific conclusions for the applicability of the  $i$ - $T$ - $\eta$  curve in predicting the voiding behavior of industrially plated Cu samples. In addition to this, the qualitative difference in the voiding behavior between the Cu samples prepared from CAPS and those generated from GPS is also unknown. To address these issues, we extend an experimental strategy used in GPS [15, 18] to the analysis of the voiding behavior of samples generated in CAPS as demonstrated in the rest of this chapter.

##### 3.1.1 Plating at ambient temperature

**3.1.1.1 Chronopotentiometry** In this part of the study, electroplating of Cu from CAPS was carried out at room temperature, in RDE configuration while varying the current densities from 0.8 to 30 mA cm<sup>-2</sup>. The potential transients for the first 5,000 s of growth are shown in Fig. 1. As demonstrated previously in the GPS studies, the potential transient shape is a good indicator for predicting a change in the growth conditions and resultantly an alteration of the voiding propensity [13–15]. However, owing to the proprietary CAPS chemistry, a significant challenge is encountered when to correlate the potential transient shape to the voiding propensity in the current study. Nonetheless, relying on an earlier shown qualitative similarity in both, potential transient shape and general trend in the voiding behavior with samples plated in GPS containing PEG + SPS + Cl<sup>-</sup> [14], we have a strong reason to believe that CAPS additives contain both, suppressor and brightener, likely PEG and SPS, respectively or their substitutes. Furthermore, since determining the chemical formula for the additives in CAPS is not the concern of this study, for the sake of this analysis, we are herein considering that CAPS also contains PEG and SPS as additives.

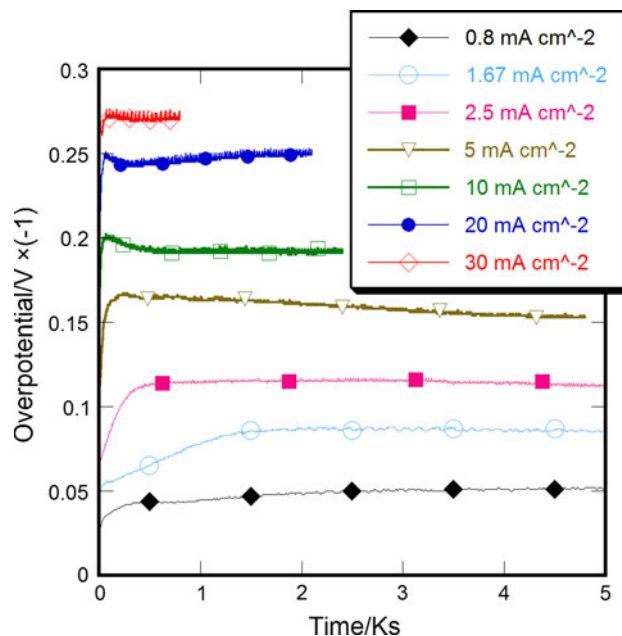


**Fig. 1** Potential transients of Cu plated in CAPS using RDE from current densities of 0.8–30 mA cm<sup>-2</sup> and at ambient temperature (Note only the potential transients for the first 5,000 s of growth or less are presented)

As seen in Fig. 1, the analysis of the potential transients obtained at current density of 10 mA cm<sup>-2</sup> or higher suggests the establishment of a specific transient shape characterized by initial decrease, followed by an increase that eventually reaches a steady state. The current density of 10 mA cm<sup>-2</sup> was chosen because of (i) its relevancy to most of the industrial plating protocols and (ii) its suitability in demonstrating temperature-driven voiding trends [15, 18]. Comparing the magnitude of potential increase observed for CAPS in Fig. 1 with the one obtained from the GPS solution of PEG + SPS + Cl<sup>-</sup> [14] using the growth rate at 10 mA cm<sup>-2</sup> as an example, one can clearly see that the former is minimal (less than 0.01 V) versus around 0.05 V for the latter. The observed potential increase is found to be as the result of a gradual displacement on the growing Cu surface of the rapidly formed PEG-Cl<sup>-</sup> complex by the SPS-Cl<sup>-</sup> one [14, 20]. Therefore, the large difference in the potential increase indicates that there must be a variation in the composition of organic additives between these two solutions while all other plating conditions remain the same. This variation is most likely represented by a difference in the suppressor to brightener ratio or PEG to SPS ratio in particular as it has been shown that a higher PEG to SPS ratio favors a more rapid formation of PEG-Cl<sup>-</sup> layer on the growing Cu surface [6]. If we assume based on potential transient comparison a higher value for the PEG:SPS ratio in GPS, then the CAPS plating would feature less pronounced competition between PEG + Cl<sup>-</sup> and SPS + Cl<sup>-</sup>, and the potential transient of CAPS shown

in Fig. 1 would resemble the one for GPS containing SPS +  $\text{Cl}^-$  (i.e., an initially increase in the potential, followed by a steady state [14]). It could be speculated that a reason for adding more SPS has something to do with the fast depletion of SPS during the plating [6]. Thus, a higher SPS concentration would provide longer plating without the need for additive replenishments. Furthermore, the potential transients for plating rate at  $5 \text{ mA cm}^{-2}$  or lower do not feature the potential increase at the beginning of the plating, instead a potential decay is observed that is closely similar to the potential transient for the plating in GPS containing only SPS +  $\text{Cl}^-$ , strengthening the argument for a lack of competition between PEG- $\text{Cl}^-$  and SPS- $\text{Cl}^-$ . One can therefore deduce that there are either fewer suppressors or the suppressors' adsorption is weaker for the lower plating rates (overpotentials positive than  $-0.16 \text{ V}$ ).

**3.1.1.2 Voiding propensity** Figure 2 shows cross sections of solder joints with Cu electroplated in the experiment analyzed in the previous section. While no sample is completely void free in Fig. 2, a trend in the voiding propensity as a function of the plating rate is clearly seen. A continuous and thick layer of voids in the  $\text{Cu}_3\text{Sn}$  intermetallic layer observed for current densities of 0.8 and  $1.7 \text{ mA cm}^{-2}$  gradually shrinks to a line of voids for 2.5 and  $5 \text{ mA cm}^{-2}$  and then transform itself into a set of separated voids with decreasing density at plating rates

exceeding  $10 \text{ mA cm}^{-2}$ . These results overall are qualitatively comparable (as trend) to findings of our previous studies [14] on GPS-plated Cu where a relatively thin layer of voids was observed at current densities less than  $2 \text{ mA cm}^{-2}$ , separate voids were found for plating in the range  $2\text{--}10 \text{ mA cm}^{-2}$ , and virtually no voiding was seen at current densities above  $10 \text{ mA cm}^{-2}$ . In general, with that set of cross-sectioned samples, we obtain a solid qualitative trend manifested by a very high level of voiding in the  $\text{Cu}_3\text{Sn}$  IMC that gradually almost disappears at a lower overpotential and higher plating rate, respectively. The registered identical voiding trend here, suggests similar key additives operating in both CAPS and GPS (i.e., PEG, SPS, and  $\text{Cl}^-$  ions or their substitutes). Given similarity of the plating chemistry, no substantial difference in the voiding trends registered in both solutions could be expected within the realm of changing current density only. However, a careful comparison of both experiments (GPS and CAPS plating) shows that the GPS plated samples are generally less prone to voiding. Comparing the voiding behavior presented in Fig. 2 to the one of samples deposited in GPS containing SPS + PEG +  $\text{Cl}^-$ , one sees a significant decrease in the overpotential where the voiding as a first approximation disappears in the CAPS solution,  $-0.20$  vs.  $-0.11 \text{ V}$  as shown in our previous study [14, 15, 18]. It is also true that even at overpotential of  $-0.20 \text{ V}$  (current density of  $10 \text{ mA cm}^{-2}$ ), the voiding propensity has not

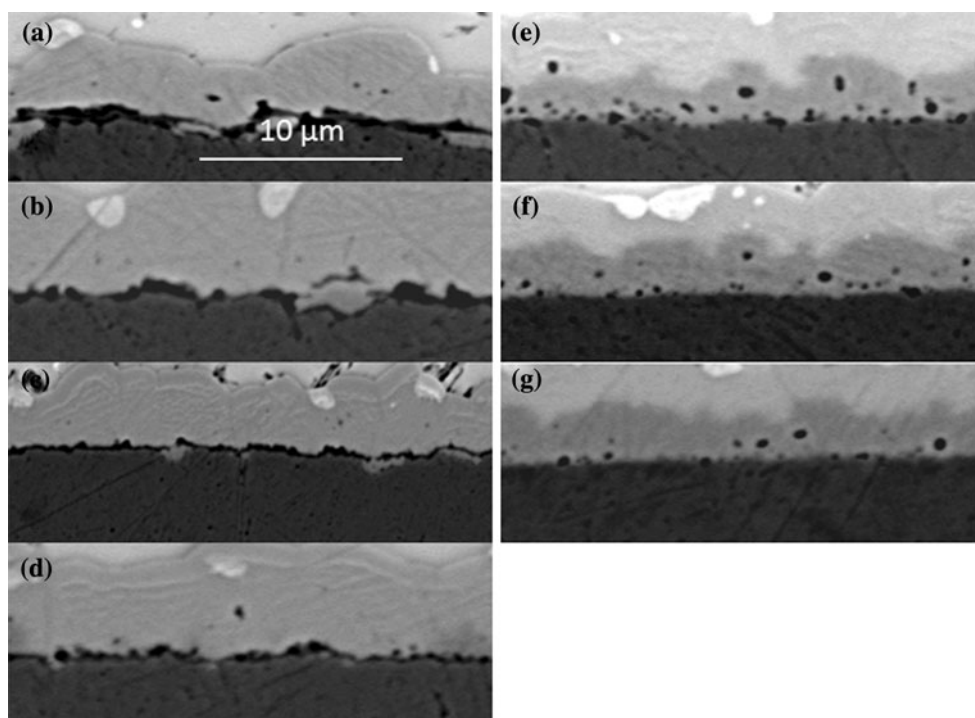


**Fig. 2** SEM micrographs of solder joint cross sections for Cu plated in CAPS using RDE at ambient temperature and at current densities of **a** 0.8, **b** 1.7, **c** 2.5, **d** 5, **e** 10, **f** 20, and **g**  $30 \text{ mA cm}^{-2}$

disappeared completely and a few voids are still seen in the  $\text{Cu}_3\text{Sn}$  IMC. This observation is most likely due to some differences in the concentration ratio between the suppressor and brightener in both cases as it was pointed out in the previous section. Also, as reported in our previous study [13, 14], the void-free copper is produced only when a delicate balance between the suppressor and brighter in concentration helps prevent the incorporation of either compound. This means that a higher SPS to PEG ratio in CAPS would likely disrupt this balance, leading to the possible incorporation of more SPS molecules and resulting in the formation of more voids. Once again, the exact reason for the difference in the void level remains unclear given the fact that the detailed composition of CAPS is unknown and besides PEG and SPS, any other additives present may impact one way or another the delicate suppressor–brightener balance and in turn the voiding propensity of accordingly plated Cu layers.

### 3.1.2 Plating at constant current density of $10 \text{ mA cm}^{-2}$

#### 3.1.2.1 Chronopotentiometry

The effect of overpotential to sulfur-containing additive adsorption, for example, SPS, has been recently studied [6]. It is reported that SPS adsorption in the growth Cu is rapidly consumed from the plating bath at high overpotentials, and the result of this consumption is manifested by the incorporation of S-containing products in the growing Cu layer. From our recent studies [15], we demonstrated that at high overpotentials, sudden precipitation of  $\text{CuCl}$  could bond a good portion of the free  $\text{Cl}^-$  ions that in turn would weaken the adsorption of  $\text{PEG} + \text{Cl}^-$  complex. As a result of this weakening, the relative impact of the SPS adsorption would increase. Knowing that these additives compete for the adsorption sites with  $\text{PEG} + \text{Cl}^-$  dominating in the initial stage in covering the Cu surface to establish eventually the delicate balance warranting the deposition of void-free Cu [6], the dynamics generated by possible precipitation of  $\text{CuCl}$  could eventually compromise the entire trend and thereby enable the incorporation of SPS- and/or S-containing products.

In the experiments described in this section, we monitor the plating kinetics and evolution of voids in the  $\text{Cu}_3\text{Sn}$  layer as a function of temperature in Cu plating runs at a fixed current density of  $10 \text{ mA cm}^{-2}$  where the overpotential of  $-0.180 \text{ V}$  warrants the deposition of moderately void-prone Cu at ambient conditions. Specifically, by varying temperature, Cu was plated galvanostatically in CAPS and the registered plots of overpotential versus time are shown in Fig. 3. Assuming the presence of SPS and PEG as key additives in the CAPS solution, the results presented in Fig. 3 suggests fast establishment of a steady-state potential in most of the curves implying the absence of initial adsorption

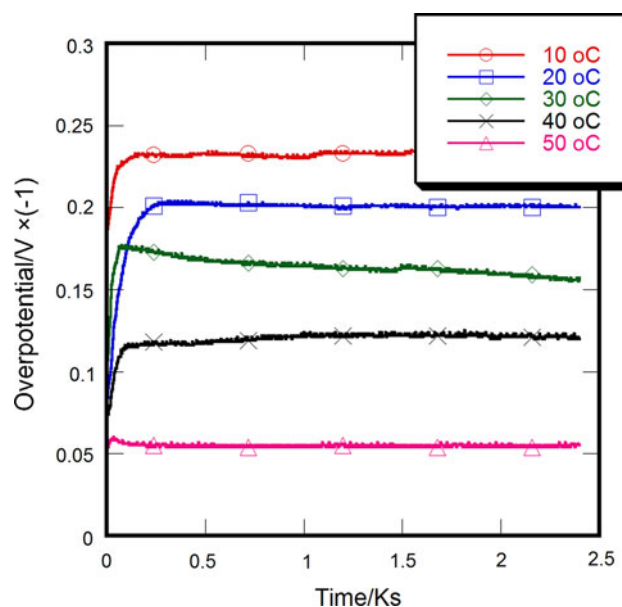


**Fig. 3** Potential transients of Cu plating in CAPS at a current density of  $10 \text{ mA cm}^{-2}$  in the temperature range of 10–50 °C

competition between the SPS and PEG complexes. Based on the relatively high overpotential registered in these runs, it could be speculated that the dominant adsorbent would be the S-containing additive relative to the glycol-containing additive that is weakly adsorbed. Overall, compared to our previous results, the overpotentials for Cu plating from CAPS at a current density of  $10 \text{ mA cm}^{-2}$  are just slightly lower to those obtained for Cu plating from GPS containing SPS + PEG +  $\text{Cl}^-$  at this current density [14, 15].

#### 3.1.2.2 Voiding propensity

SEM images for the samples plated in CAPS with RDE at 50 RPM and studied electrochemically in the previous section are shown in Fig. 4 below. From these images, it is clear that at high overpotential of  $-0.05 \text{ V}$  and high temperature of 50 °C Fig. 4e, there is a thick layer of voids, while isolated voids are evident in the  $\text{Cu}_3\text{Sn}$  at lower overpotentials ranging from  $-0.20$  to  $-0.23 \text{ V}$ , and low temperatures of 10 and 20 °C, respectively (Fig. 4a, b). The observed lower overpotentials registered would correlate with better balance between S-containing and glycol-containing additives in the case considered resulting to small and isolated voids in the  $\text{Cu}_3\text{Sn}$  layer as per our reported previous results [13–15]. A few small spheres of voids were still visible as shown in Fig. 4a and b for experiments that were carried out at temperatures of 10 and 20 °C, respectively. This trend is qualitatively similar to our previous results [14, 15] where the GPS (SPS + PEG +  $\text{Cl}^-$ ) Cu plating solution had been used instead of CAPS. As mentioned earlier, however, the quantitative difference in the voiding propensity in both cases may be attributed to unknown additives in the CAPS

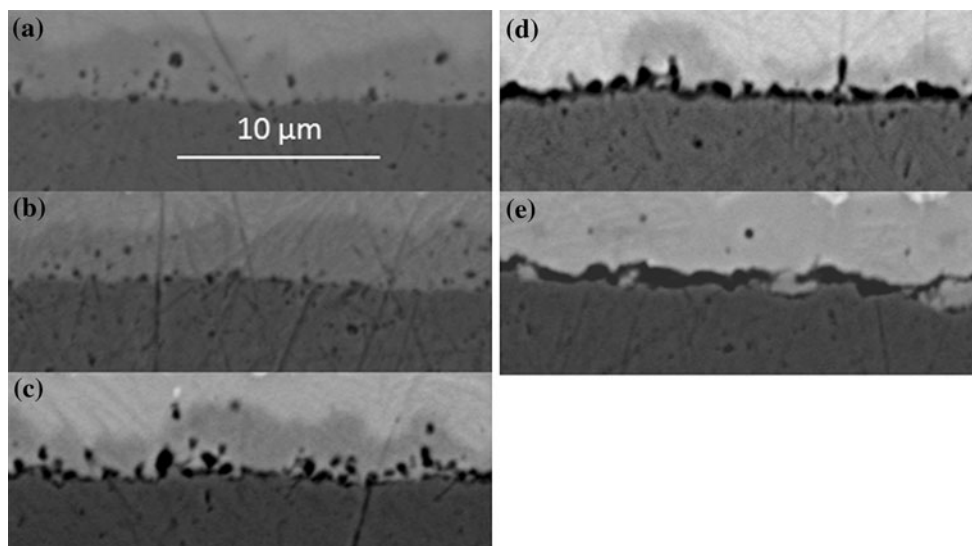


**Fig. 4** SEM micrographs of solder joint cross-section for Cu plated in CAPS at a current density of  $10 \text{ mA cm}^{-2}$  and at solution temperatures of **a** 10, **b** 20, **c** 30, **d** 40, and **e** 50 °C

bath. Comparing these results with those carried out at room temperature but at different current densities (Sect. 3.1.1), one sees that the magnitude of voiding is almost comparable for the samples plated within identical overpotential ranges. Summarized results of this comparison are presented in the next section.

### 3.1.3 $I$ – $T$ – $\eta$ dependences

Following the analysis presented in our earlier article [15], it is important to generate a quantitative plot of  $i$ – $\eta$  and  $T$ – $\eta$  to identify the overpotential ranges within which growth Cu is found to be void prone or void proof. A summary for such dependencies derived from the results discussed above is as shown in Fig. 5 below. The comprehensive overview of the  $i$ – $\eta$  and  $T$ – $\eta$  plots along with the SEM images presented in Figs. 2 and 4 clearly suggests that with the increase in the overpotential, the level of voiding in the IMC continuously increases. This result is qualitatively similar to the overall trend reported recently for our GPS Cu plating bath containing SPS + PEG +  $\text{Cl}^-$  [15, 18] whereby overpotentials of  $\sim -0.11 \text{ V}$  or more are favorable for the production of “void-prone” Cu. Also, if we take as a rough approximation that the isolated voids in the last two images of Fig. 2 and the first two images in Fig. 4 represent a virtually void-free interface, we can conclude that a substantial voiding in Cu layers deposited from CAPS are obtained in the range of overpotentials of  $\sim -0.20 \text{ V}$  or more regardless of the growth protocol employed. The quantitative difference in the voiding propensity in layers grown from both plating baths could be attributed mainly to minor compositional differences between the two plating baths. As described earlier in this

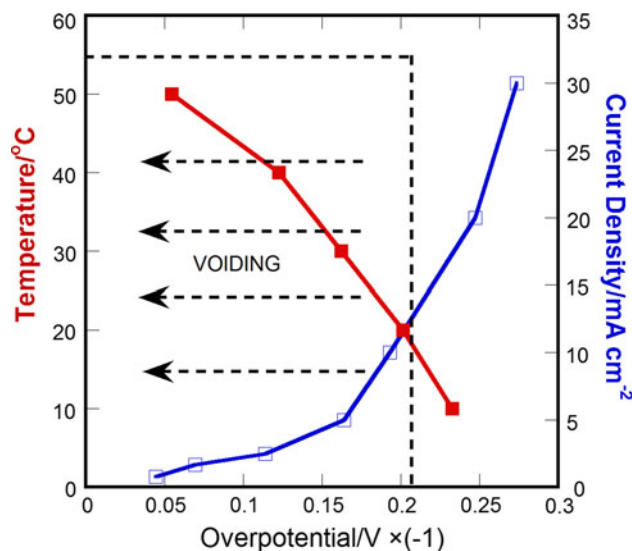


**Fig. 5** Quantitative trends in the voiding propensity with respect to solution temperature, deposition rate and deposition potential in CAPS

article, we speculated that these differences are quantitative and are most likely represented by a lower PEG:SPS ratio in the CAPS solution.

### 3.2 Voiding behavior of Cu plated in Hull cell

After carrying out a comprehensive analysis of the voiding behavior of Cu plated on 6-mm disks in RDE configuration in both CAPS (this study) and GPS [13–15], scale-up experiments are performed in a Hull cell featuring a volume of 267 mL and designed in a way that the cathode panel on one end is close to the anode only separated by a

distance of 5 cm while the other end of the cathode panel far from the anode is separated by a distance of 12 cm. The main focus of these experiments is on the spatial distribution of the voiding propensity produced by the inhomogeneity of the electric field of the Hull cell configuration and the applicability of the analysis proposed in [15] and earlier in this article for assessment of the possibility for voiding as a function of locally operating plating parameters. More specifically, the Hull cell design produces an uneven thickness of the deposit [21] as different spots across the cathode do not experience the same magnitude of the electric field. This is as a result of the lower IR impact when the cathode is closer to the anode leading to a higher current and vice versa. Local current density calculations were made by measuring the local thickness of the deposited layer,  $\Delta$ , and taking into account Eq. 1 that could easily rearrange in a way to be solved for  $i$  [22]

$$t = \frac{zFd\Delta}{AW \times i} \quad (1)$$

where  $t$  time (s),  $\Delta$  thickness of the deposit (cm),  $z$  number of exchanged electrons ( $z_{\text{Cu}} = 2$ ),  $F$  Faraday's constant ( $9,6500 \text{ C mol}^{-1}$ ),  $d$  density of metal deposit ( $\text{g cm}^{-3}$ ),  $AW$  atomic weight of the depositing metal ( $\text{g mol}^{-1}$ ), and  $i$  current density ( $\text{A cm}^{-2}$ ). After plugging in the constants and rearranging of Eq. 1 above, a simplified form of the equation is obtained as shown below;

$$i = 27211 \frac{\Delta}{t} \quad (2)$$

### 3.2.1 Voiding of Cu plated in GPS

**3.2.1.1 PEG +  $\text{Cl}^-$  system** (a) *Sample preparation*: In our most recent study, we have reported that for Cu that is plated at ambient temperature from the acidic Cu plating bath with PEG +  $\text{Cl}^-$  additives, the incorporation of impurities take place at overpotentials lower than  $-0.23 \text{ V}$ , and this in essence translates to higher current densities [15, 18]. We also reported that at these higher overpotentials, the catalytic effect of the  $\text{Cl}^-$  ions is more favorable for keeping large PEG molecules on the Cu surface [15], thereby raising the odds for higher rate of impurity incorporation. The plating of Cu was done at room temperature, and an average current density of  $10 \text{ mA cm}^{-2}$  was applied. It should be noted that, in these experiments, the electrodeposition of Cu was carried out in a stagnant electrolyte (no stirring), and the long-term solid-state aging after soldering for these samples was carried out for 168 h. The current density across the cathode was determined according to the procedure described earlier in this article and found to range from  $8.6$  to  $19.1 \text{ mA cm}^{-2}$ .

(b) *Voiding propensity, horizontal cross-section of the cathode panel*: Soldering on the electroplated cathode panel

was done in both horizontal rows and vertical columns, as shown in the schematic diagram below (Fig. 6). Owing to the specific geometry of the Hull cell, the part of cathode surface that is close to the anode should be subjected to a higher current. Figure 7 shows the SEM images of solder joint cross-sections for the Cu grown in the PEG +  $\text{Cl}^-$  solution in a Hull cell. Analyzing results obtained from this system, it is clear from Fig. 7a–c that at high current densities, a thick layer of voids is formed on the  $\text{Cu}_3\text{Sn}$  interface. On the other hand, at low current densities, we have isolated voids to no-voids situation, as shown in Fig. 7d–f. It is clear that the areas that are closer to the anode and thereby experience stronger electric field during the Cu plating process feature higher level of voiding in the  $\text{Cu}_3\text{Sn}$ . The reasons explaining this observation were discussed in detail in our previous study [13–15, 18]. In general, in such a case, the voiding propensity steadily increases with the plating rate. The transition between the regions of “void-prone” to “void-proof” Cu on the same cathode panel in the Hull cell experiments with PEG +  $\text{Cl}^-$  is observed between  $9.6$  and  $8.6 \text{ mA cm}^{-2}$  as shown in Fig. 7e, f, while in the experiments carried out in RDE configuration from the same plating bath composition, this transition was observed between the current density of  $1.7$  and  $0.5 \text{ mA cm}^{-2}$  [13]. The discrepancy can be attributed most likely to a faster aging of the Hull cell solution warranted by the almost an order of magnitude higher electrode surface to solution volume ratio. More specifically in the RDE experiments, the volume of the bath is  $50 \text{ mL}$  while the surface area of the electrode is  $0.28 \text{ cm}^2$  compared to the  $267 \text{ mL}$  and  $46 \text{ cm}^2$ , respectively for experiments done in the Hull cell. Despite the quantitative differences, both sets of results are qualitatively (as trend) in agreement in both cases featuring a steadily increasing voiding propensity with the increase of the current density applied for the electrodeposition of Cu in the PEG +  $\text{Cl}^-$  solution. As it was discussed elsewhere [13–15], higher currents in this solution run at overpotentials where the incorporation of impurities in the growing Cu layer is favorable. Once incorporated above some critical level, these impurities block the vacancy annihilation

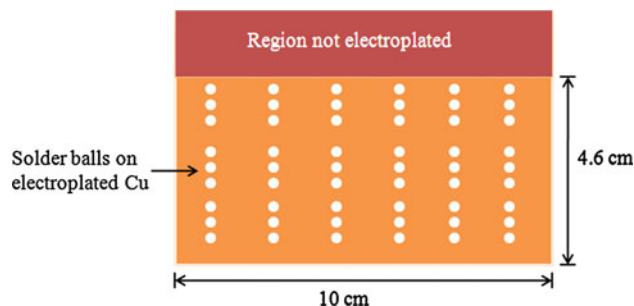


**Fig. 6** A schematic diagram showing balling electroplated cathode panel used in the Hull cell experiments



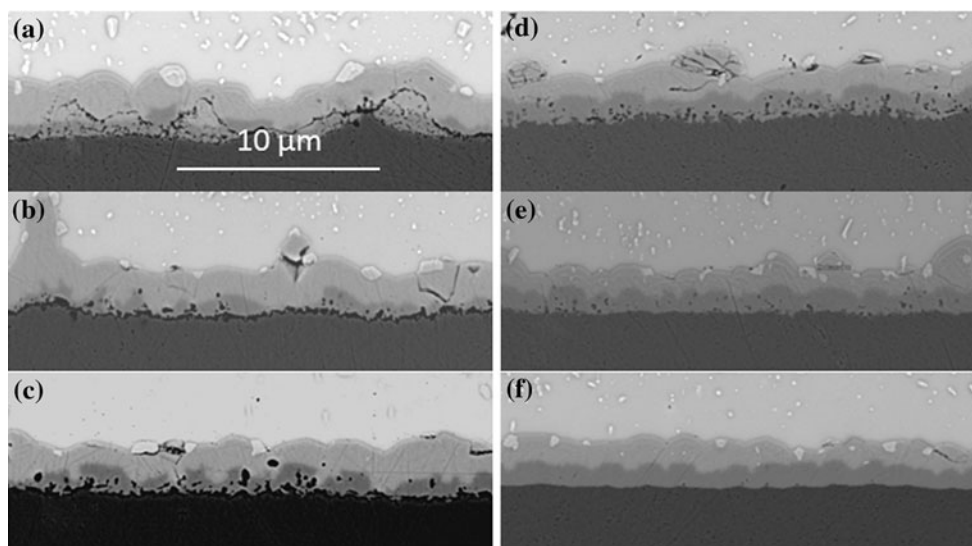


**Fig. 7** SEM micrographs of solder joint cross-section for Cu plated in PEG +  $\text{Cl}^-$  solution in a Hull cell at ambient temperature with calculated current densities of **a** 19.1, **b** 17.3, **c** 13.1, **d** 10.8, **e** 9.6, and **f** 8.6  $\text{mA cm}^{-2}$

sites and as a result of all that a vacancy supersaturation leads to nucleation and growth of larger in size voids or that in some cases could merge into layers of voids.

(c) *Voiding propensity, vertical cross-section of the cathode panel:* SEM images from another cross sectioning of the same cathode panel considered in the previous section are presented in Fig. 8. However, this time the cross sectioning was done vertically and comprised the cathode end that was closer to the anode. The analysis of the SEM images suggests a decrease in the thickness of the electroplated Cu on the cathode from the bottom to the top of the column. Also, voiding propensity was generally decreasing with the sample at the bottom showing massive voiding, Fig. 8a that degrades to isolated voids at the sample top, as seen in Fig. 8d. The most plausible explanation of this result could be associated with the presence of a vertical concentration gradient established owing to gravitational reasons. More recent experiments carried out

in a stirred solution (not shown here) demonstrate minimization to complete disappearance of the vertical voiding trend thus confirming the gradient hypothesis.

**3.2.1.2 SPS + PEG +  $\text{Cl}^-$  system** We reported recently that the voiding propensity for Cu samples plated in SPS + PEG +  $\text{Cl}^-$  acidic bath is higher at low current densities [14, 15]. Since it is well documented that the voiding is correlated with impurity incorporation [13, 14], low current densities specifically favor the impurity incorporation when plating is carried out in the SPS + PEG +  $\text{Cl}^-$  system. As we recently reported, there is weak adsorption of PEG complexes at low overpotentials (low current density) because of precipitation of CuCl that bonds most of the free  $\text{Cl}^-$  ions. This eventually strengthens the adsorption of SPS complexes and compromises the balance with PEG to favor (as a result) the incorporation of S-containing compounds and enhance the voiding [15]. Other

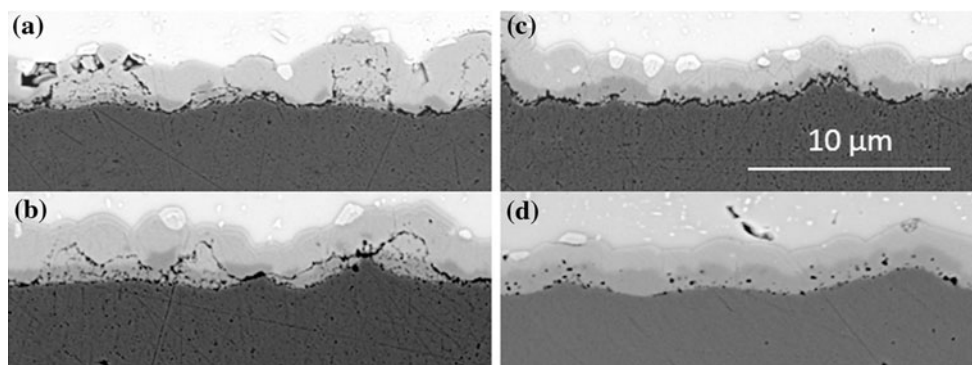


**Fig. 8** SEM micrographs of solder joint cross-section for Cu plated in PEG +  $\text{Cl}^-$  solution in a Hull cell at ambient temperature with calculated current densities of **a** 19.1, **b** 16.0, **c** 13.0, and **d** 9.9  $\text{mA cm}^{-2}$

studies have shown that in the presence of SPS, there is a high S segregation on the Cu/Cu<sub>3</sub>Sn interface and void surface, suggesting that segregation of S to the Cu/Cu<sub>3</sub>Sn interface lowered interface energy and thereby the free energy barrier for Kirkendall voids nucleation [8, 11, 12]. Our previous study has demonstrated that the voiding propensity in 10 μm of Cu electroplated on 6-mm Cu disks in RDE configuration decreases with the increase of the current density [14]. These results serve as a reference point in the choice of deposition current density for the Hull cell experiments. Figure 9 summarizes the results obtained by Cu plating at average current density of 5 mA cm<sup>-2</sup>. It is clearly seen that the voiding propensity becomes almost negligible at current densities of 10 mA cm<sup>-2</sup> or above (Fig. 9a, b) whereas a substantial voiding is seen at the lower end of plating rates (Fig. 9d, e). Compared to the results obtained on 6-mm disks in RDE configuration [14], the results in Fig. 9 associate a higher current density with the voiding disappearance. However, the trend in voiding is qualitatively identical and confirms the growth of void-prone Cu at generally low overpotentials where SPS adsorbs stronger compared to PEG. Also, comparing the SEM images in Figs. 7 and 9, one observes opposite trends of voiding versus the deposition current density. This observation emphasizes one more time the key difference in the voiding behavior of samples grown in different plating baths. Even though the voiding propensity in the Hull cell and RDE configuration only qualitatively (or semi-quantitatively) identical, the general similarity of the voiding behavior enables a new level of control and anticipation of the voiding behavior in larger scale plating environment. At the same time, the quantitative differences in the transitional current densities/overpotentials are mostly

attributed to the dynamics of the additive consumption in different plating baths, which is clearly demonstrated by a more rapid SPS consumption leading to enhanced voiding in Cu deposits grown in the Hull cell setup. A future study is designed to investigate and elaborate in detail on the aging effect associated with the difference in the substrate surface to plating volume ratios.

### 3.2.2 Voiding of Cu plated in CAPS

A Hull cell was also used to study the current density effect on the voiding when Cu plating was carried out in the CAPS. Average current densities of 2 and 7 mA cm<sup>-2</sup> were applied in two separate Cu plating experiments. These current densities were chosen based on our previous studies [14, 15, 18], in a way that would presumably provide across the cathode panel the entire voiding spectrum ranging from void-proof to void-prone Cu. The first part of the experiment was aimed at using higher current density of 7 mA cm<sup>-2</sup> and (in turn) providing for the deposition of low-voiding to void-free Cu samples. In the second experiment a low current density of 2 mA cm<sup>-2</sup> was applied as this was aimed at shifting the overpotential positively and (in turn) at raising the odds for observing high levels of voiding propensity. SEM images of the horizontal cross-sectioning of the plated, soldered, and aged cathode panels from these experiments are shown in Fig. 10. The analysis of the SEM images presented in Fig. 10, unambiguously demonstrates a trend manifested by enhanced voiding propensity at the very low current densities (Fig. 10e, f) and vice versa, almost non-existing voids at the highest current densities (Fig. 10a, b). These

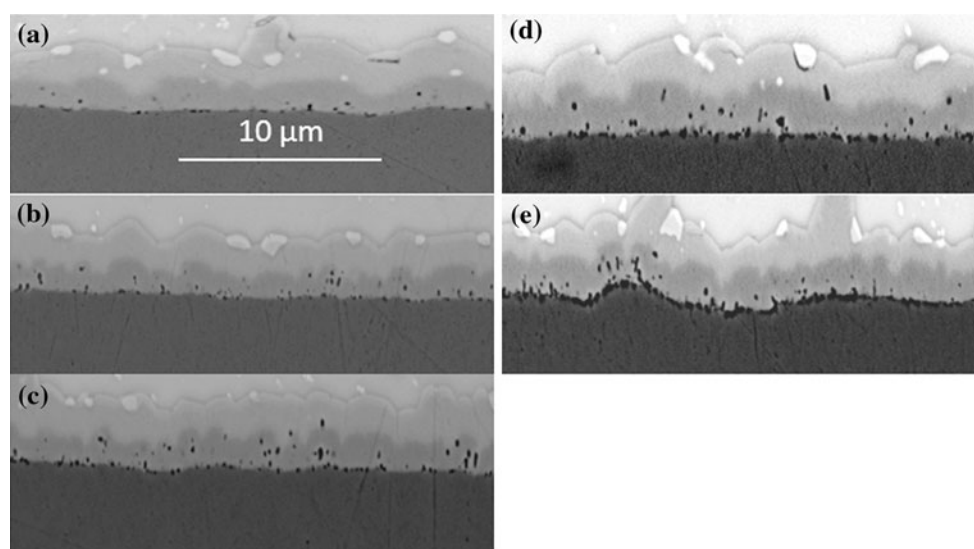


**Fig. 9** SEM micrographs of solder joint cross-section for Cu plated in SPS + PEG + Cl<sup>-</sup> solution in a Hull cell at ambient temperature with calculated current densities of **a** 12.1, **b** 9.9, **c** 7.6, **d** 5.3, and **e** 4.3 mA cm<sup>-2</sup>

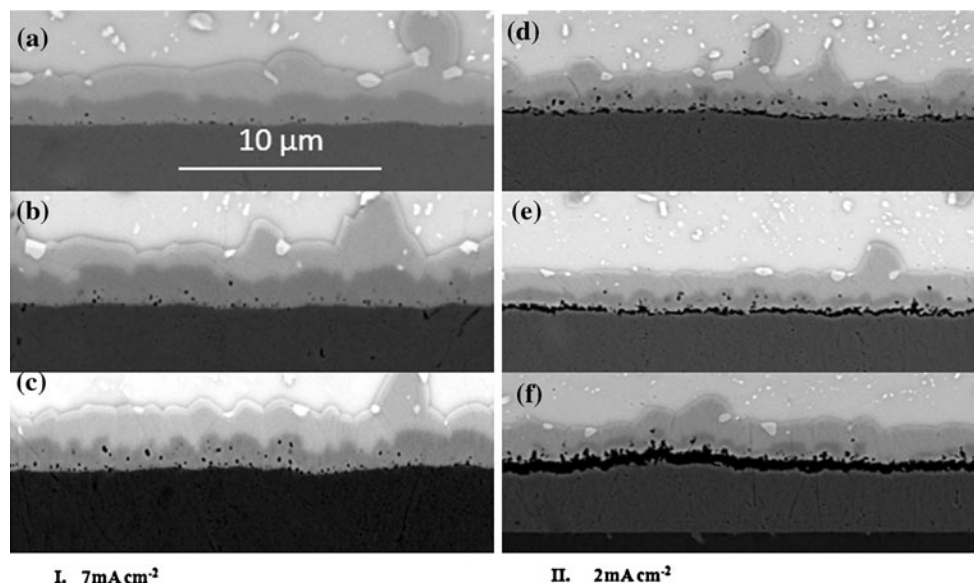


**Fig. 10** SEM micrographs of solder joint cross-sections for Cu plated in a CAPS solution in a Hull cell at 25 °C, and at an average current density of (I) 7 mA cm<sup>-2</sup> and (II) 2 mA cm<sup>-2</sup>. The calculated local current densities were **a** 14.2, **b** 12.2, **c** 7.2, **d** 5.2, **e** 2.9, and **f** 1.5 mA cm<sup>-2</sup>

scaling up experimental results are virtually identical with those obtained when Cu was electroplated from CAPS using the RDE at 50 RPM as described in Sect. 3.1 above. This finding implies lower sensitivity of the experiments carried out in CAPS to surface area and plating volume as compared to plating runs using GPS. We can just speculate that this could be due to a higher concentration of the S-containing additive in the CAPS formulation that would provide steadier plating conditions for a longer time. Also the voiding trend registered in Fig. 10 confirms one more time the qualitative similarity between our GPS (SPS + PEG + Cl<sup>-</sup>) and the CAPS examined in this study. It may be interesting in the future to study in a similar way more brands of CAPS and identify specific similarities and differences.

#### 4 Conclusions

A quantitative study of the impact of key Cu plating parameters on the voiding propensity of solder joints with Cu electroplated in CAPS performed on 6-mm diameter Cu disks in RDE configuration demonstrates a decreasing trend of the voiding propensity with an increase of the overpotential applied. It also identified the range of overpotentials negative to -0.20 V as best for depositing void-proof Cu. The CAPS voiding trends are found to be qualitatively similar to GPS (SPS + PEG + Cl<sup>-</sup>) used in this and in other studies of our group. In the second part of this article, the study of the voiding propensity in solder joints with Cu electrodeposited in Hull cell in both, generic

plating solution (GPS) and CAPS demonstrates clearly the plating of co-existing on the same panel void-prone and void-proof Cu. While generally confirming the qualitative trends registered in the experiments carried out in RDE configuration, the experiments performed in a Hull cell reveal effects pointing out toward a sensitivity of the plating protocols to the ratio of surface area to plating volume. More specifically, lower values of this ratio lead to slower consumption of the additives which in turn warrants plating parameter to operate after longer aging for plating in RDE configuration. The results of this study represent a step ahead in the development of better understanding on the voiding in industrial Cu plating environment and clearly illustrate for the first time the co-existence of void-prone and void-proof Cu thus elaborating further on the sporadic nature of the voiding phenomenon.

**Acknowledgments** The authors of this study acknowledge the financial support of the IEEC at Binghamton University. ND, FW, and YL acknowledge also the partial support by the National Science Foundation, Division of Materials Research (DMR-0742016).

#### References

1. Chiu T, Zeng K, Stierman R et al (2004) In: The proceedings of the 54th electronic components and technology conference. IEEE, p 1256
2. Zeng K, Stierman R, Chiu T et al (2005) J Appl Phys 97:024508
3. Mattila TT, Kivilahti JK (2005) J Electron Mater 35:250
4. Borgesen P, Yin L, Kondos P et al (2007) In: The proceedings of the 57th electronic components and technology conference. IEEE, p 136

5. Andricacos PC, Uzoh C, Dukovic JO et al (1998) *IBM J Res Dev* 42:567
6. Moffat TP, Wheeler D, Edelstein MD et al (2005) *IBM J Res Dev* 49:19
7. Yin L, Kondos P, Borgesen P et al (2009) In: The proceedings of the 59th electronic components and technology conference. IEEE, p 406
8. Kim JY, Yu J, Kim SH (2009) *Acta Mater* 57:5001
9. Laurila T, Vuorinen V, Kivilahti JK (2005) *Mater Sci Eng* 49:1
10. Yang W, Messler RW (1994) *J Electron Mater* 23:765
11. Yu J, Kim JY (2008) *Acta Mater* 56:5514
12. Kim JY, Yu J (2008) *Appl Phys Lett* 92:092109
13. Liu Y, Wang J, Yin L et al (2008) *J Appl Electrochem* 38:1695
14. Liu Y, Yin L, Bliznakov S et al (2010) *IEEE Trans Compon Packag Technol* 33:127
15. Wafula F, Liu Y, Yin L et al (2010) *J Electrochem Soc* 157:D111
16. Vereecken PM, Binstead RA, Deligianni H et al (2005) *IBM J Res Dev* 49:3
17. Gabrielli C, Mocoteguy P, Perrot H et al (2007) *J Electrochem Soc* 154:D13
18. Wafula F, Liu Y, Yin L et al (2009) *ECS Trans* 19:43
19. Vukmirovic MB, Vasiljevic N, Dimitrov N et al (2003) *J Electrochem Soc* 150:B10
20. Moffat TP, Wheeler D, Josell D (2004) *J Electrochem Soc* 151:C262
21. Hull RO (1939) *Proc Am Electroplat Soc* 27:52
22. Schlesinger M, Paunovic M (2000) *Modern electroplating*, 4th edn. Wiley Interscience, New York, pp 14–16